Comparative study of thermal and photo-induced reactions of NO on particulate and flat silver surfaces

Ki Hyun Kim [a,1], Kazuo Watanabe [a,2], Dietrich Menzel [a,b,*], Hans-Joachim Freund [a]

[a] Fritz-Haber-Institut der Max-Planck-Gesellschaft, Faradayweg 4–6, 14195 Berlin, Germany
[b] Physik-Department E20, Technische Universität München, 85748 Garching, Germany

ARTICLE INFO

Article history:
Received 29 August 2011
Accepted 6 February 2012
Available online 20 February 2012

Keywords:
Silver nanoparticles
Photon stimulated desorption
Plasmon excitation
Confinement of excitations
Nitric oxide

ABSTRACT

Adsorption states, thermal reactions, and photoreactions at photon energies 2.3–4.7 eV of NO dimers and monomers have been compared between 8-nm silver nanoparticles (Ag NPs) formed on an Al_2O_3/NiAl(110) substrate and flat Ag(111) surfaces, by thermal desorption (TPD) and by photodesorption using mass selected time-of flight measurements. On the Ag NPs, the $(NO)_2$ and NO species are bound more weakly and with broader variation of adsorption states, compared to Ag(111). For $(NO)_2$ excitation of the Mie plasmon of the Ag NPs with *p*-polarized 3.5-eV photons enhances the photodesorption cross section (PCS) of NO from $(NO)_2$ by a factor 15 compared to Ag(111); even off the plasmon resonance up to 3-fold PCS enhancement is obtained which we ascribe to hot electron confinement. However, since translational energy distributions of photodesorbed NO are roughly the same on Ag NPs and on Ag(111), common mechanisms of photoexcitation and photoreactions apply on both types of surfaces, and neither enhancement modifies the photoinduced dynamics. Stronger particle-induced influences are observed for the photoinduced NO monomer by changes in its properties, chemical environments, and formation/decay kinetics.
Our results show that NPs can lead to considerable changes of efficiency and, under favorable cases, also of branching of photoinduced surface reactions.

1. Introduction

Motivated by demands for more efficient catalysts and by the fundamental interest in the new phenomena becoming important for small aggregates of atoms, techniques to fabricate and characterize metal clusters (MCs, particle diameter $d<\sim 1$ nm) or metal nanoparticles (MNPs, $d>\sim 1$ nm) supported on solid surfaces have been developed in the last two decades in order to study elementary chemical processes on surfaces of catalysts.[3] Surface analytical methods such as XPS (X-ray photoelectron spectroscopy) and other spectroscopies, and STM (scanning tunneling microscopy) or other microscopies are employed, making molecular and atomistic information on surface chemical reactions accessible.

Photoreactions on MNPs prepared on well defined solid surfaces are relatively new research topics compared to thermal reactions. The interplay of unique optical properties[4] and changed electron dynamics of MNPs[5] as well as their specific surface morphologies can significantly modify both elementary and overall photochemical processes compared to extended systems.[6] For example, the excitation of the particle plasmon (Mie)[7] resonance has been shown to enhance photoreactions of NO on silver nanoparticles,[8] and the quantum efficiency of photodesorption was shown to increase with decreasing particle size.[9] The branching ratio of photoreactions of methane on Pd NPs changes with particle size.[10] Hyperthermal photodesorption of Xe atoms can be induced by plasmons due to electronic repulsion.[11] These phenomena are potentially useful for development of more efficient and tailor-

* Corresponding author at: Physik-Department E20, Technische Universität München, 85748 Garching, Germany. Tel.: +49 8928912616; fax: +49 8928912338.
E-mail address: dietrich.menzel@ph.tum.de (D. Menzel).
[1] Present affiliation: Korea Photonics Technology Institute, 5 Cheomdan 4gil, Buk-Gu, Gwangju, 500–779, Republic of Korea.
[2] Present address: Tokyo University of Science, 1–3 Kagurazaka, Shinjuku-ku, Tokyo 162–8601, Japan.

[3] H.-J. Freund, Chem. Eur. J. **16** (2010) 9384.
[4] U. Kreibig and M. Vollmer, *Optical properties of metal clusters*. Springer-Verlag Berlin-New York 1994.
[5] M. Quijada, R Díez Muiño, A. G. Borisov, J. A. Alonso, and P. M. Echenique, New J. Phys. **12** (2010) 053023.
[6] K. Watanabe, D. Menzel, N. Nilius, and H.-J. Freund, Chem. Rev. **106** (2006) 3014320.
[7] G. Mie, Ann. Phys. **25** (1908) 329.
[8] K. Wettergren, B. Kasemo, and D. Chakarov, Surf. Sci. **593** (2005) 235.
[9] D. Mulugeta, K. H. Kim, K. Watanabe, D. Menzel, and H.-J. Freund, Phys. Rev. Lett. **101** (2008) 146103.
[10] K. Watanabe, Y. Matsumoto, M. Kampling, K. Al-Shamery, and H.-J. Freund, Angew. Chem. Int. Ed. **38** (1999) 2192.
[11] K. Watanabe, K.H. Kim, D. Menzel, and H.-J. Freund, Phys. Rev. Lett. **99** (2007) 225501.

made photocatalysts. Indeed, photocatalysts exploiting plasmon enhancement have been reported by several groups.[12,13,14]

The purpose of the present study is to distinguish effects of particle morphology, optical properties, and electron dynamics of MNPs on photochemical processes from similar properties on flat surfaces of the bulk metals. These factors may influence adsorption states of reactants, photoexcitation probabilities, reaction paths, and energy partitioning into photoproducts. The key point of our work is to use the same experimental techniques for both MNPs and bulk metal samples prepared in the same UHV facility, and to apply them to the same system. The knowledge about photoinduced processes on surfaces of bulk single crystals accumulated in the last decades[15,16,17,18,19] can be used as basis to shed light on peculiarities induced on confined particulate metals. For this we use the photoreactions of nitric oxide (NO) molecules adsorbed on alumina supported Ag nanoparticles and on Ag(111). This is a comparatively rich system, because the low temperature necessary for NO adsorption on silver leads to the formation of NO dimers, $(NO)_2$, which have a complicated evolution both thermally and photochemically[20,21,22]: $(NO)_2$ decomposes to 2 NO part of which desorb, or to $N_2O + O$; the latter can stabilize monomeric NO. With photon energies > 2.3 eV, even hot N_2 can be formed from $(NO)_2$ by concerted scission of the two N–O bonds.[23] Our focus on differences between particulate and flat metal surfaces should offer useful implications for the potential of using nanoparticles instead of bulk materials as photocatalysts. Detailed studies of photodesorption *dynamics* for the dimer state have been published by our group recently.[24] In the present paper, we focus on the comparison of adsorption states and kinetics of photoreactions of NO between the particulate and flat Ag surfaces by using temperature programmed desorption (TPD) and photo-induced desorption (PID) with mass-selected time-of-flight (MS-TOF) measurements.

2. Experimental

All experiments have been performed in a two-level UHV system (base pressure $< 10^{-10}$ mbar) consisting of an upper sample preparation and a lower measurement chamber, separated by a gate valve.[11] Flat and particulate Ag substrates were used for comparison, namely, a Ag(111) crystal (2 mm thick, 10 mm in diameter) and Ag NPs (density ~4×10^{11} cm^{-2}) supported on a thin Al_2O_3 layer on a NiAl(110) substrate (2 mm thick, 10 mm in diameter). The mean diameter of the Ag NPs[25] was set to 8 nm in this study. Details of the sample preparations were described (in refs.[24] and[26]).

NO gas was introduced by a pulsed valve through an 8-mm copper tube ending about 3 cm in front of the sample. Prior to gas dosage, the sample was briefly heated to room temperature to remove contaminants. The sample was dosed with NO at 75 K with up to 5 L (L = Langmuir, 1 L = 1×10^{-6} Torr·s) NO to form a saturated monolayer of NO dimers. This prevents both multilayer growth and reactions of NO dimers.[9,20] Immediately after the NO dosage, the sample was cooled to ~30 K with liquid helium.

TPD (heating rate 0.5 K/s) was used to probe adsorbed molecules on the sample surface. Desorbing molecules passed a skimmer (opening 2 mm) positioned 1 mm in front of the sample and were detected by a differentially pumped quadrupole mass spectrometer (QMS). The sample was biased at −100 V to avoid electron bombardment from the QMS ionizer. QMS signals at several m/e ratios were recorded simultaneously by multiplex measurement. Signal intensities of NO^+ (m/e = 30) and N_2O^+ (m/e = 44) were corrected by their relative QMS sensitivities and the cracking patterns in the QMS ionizer. A new sample preparation was carried out prior to each set of measurements to avoid any influences of changes induced by heating and contamination.

Photoreactions of the adsorbed NO dimers were induced by irradiation with photons incident on the surface at 45º from the surface normal in *p*- or *s*-polarization at 2.3, 3.5, or 4.7 eV (the second, third, and fourth harmonics) from a nanosecond Nd:YAG laser (repetition rate at 10 Hz), or by non-polarized photons at 4.0 eV from an XeCl excimer laser. The laser fluence was 1 or 2 mJ/cm^2, depending on signal strength. At these fluences laser induced thermal processes were negligible as checked by post-irradiation TPD (see below).

Photodesorbed molecules were detected by another QMS with a LN_2 cooled ionizer at ~19 cm distance from the sample surface. TOF spectra of photodesorbed molecules were recorded by a multichannel scaler (dwell time 2 μs) triggered by the laser. A TOF spectrum was acquired for every laser pulse. The total PID yield was obtained by integrating the TOF spectra.[26] The translational energy distributions of photodesorbed molecules were obtained from the accumulated TOF spectra. The photodesorption cross section (PCS) was estimated from the decay of the PID signal as a function of photon irradiance. Details of data analysis will be described later. For further details see ref.[27]

3. Results

3.1. Pre- and post-irradiation temperature programmed desorption (TPD)

TPD has been carried out before and after photoreactions of NO on the Ag surfaces. Pre-irradiation TPD provides information about the adsorption states of NO molecules, and post-irradiation TPD on photoproducts and possible photoreaction pathways. We used identical sample preparations for pre- and post-irradiation TPD: a saturated monolayer of NO dimers was prepared on either 8-nm Ag NPs or on Ag(111). Only a monolayer is formed on Ag surfaces at this temperature,[20] and it is known[20] to consist of dimers, $(NO)_2$.

Fig. 1(a) presents TPD results for m/e = 30 from Ag NPs and Ag(111). The Ag(111) spectrum shows three peaks at 97, 115, and 400 K, originating from dissociation of NO dimers emitting gaseous NO, from NO fragments of desorbing N_2O produced by thermal reactions of NO dimers at lower temperatures, and from desorption of produced NO monomers (most likely stabilized by O adatoms).[22] Three peaks are also found in the TPD spectrum (m/e = 30) from the Ag NPs. The peak at 86 K is attributable to dissociation of NO dimers; the small peak at 102 K is assigned to NO fragments of desorbing N_2O. The broad feature between ~120 and ~450 K, consisting of two peaks at 160 K and 250 K, is attributable to desorption of NO

[12] K. Awazu, M. Fujimaki, C. Rockstuhl, J. Tominaga, H. Murakami, Y. Ohki, and T. Watanabe, J. Am. Chem. Soc. **130** (2008) 1676.
[13] K. Mori, M. Kawashima, M. Che, H. Yamashita, Angew. Chem. Int. Ed. **49** (2010) 8598.
[14] D. B. Ingram and S. Linic, J. Am. Chem. Soc. **133** (2011) 5202.
[15] D. Menzel and R. Gomer, J. Chem. Phys. **41** (1964) 3311.
[16] P.A. Redhead, Can. J. Phys. **42** (1964) 886.
[17] X. -L. Zhou, X. -Y. Zhu, and J. M. White, Surf. Sci. Rep. **13** (1991) 73.
[18] Laser Spectroscopy and Photochemistry on Metal Surfaces; H.-L. Dai and W. Ho, Eds.; World Scientific: Singapore, 1995.
[19] F. M. Zimmermann and W. Ho, Surf. Sci. Rep. **22** (1995) 127.
[20] C. I. Carlisle and D.A. King, J. Phys. Chem. B **105** (2001) 3886.
[21] S. K. So, R. Franchy, and W. Ho, J. Chem. Phys. **95** (1991) 1385.
[22] T. Vondrak, D. J. Burke, S. R. Meech, Chem. Phys. Lett. **327** (2000) 137.
[23] K. H. Kim, K. Watanabe, D. Menzel, and H.J. Freund, J. Am. Chem. Soc. **131** (2009) 1660.
[24] D. Mulugeta, K. Watanabe, D. Menzel, H.-J. Freund, J. Chem. Phys. **134** (2011) 164702.
[25] N. Nilius, N. Ernst, H. -J. Freund, Phys. Rev. Lett. **84** (2000) 3994.
[26] K. H. Kim, K. Watanabe, D. Menzel, and H.J. Freund, J. Phys.:Condens. Matter **22** (2010) 084012.
[27] K. H. Kim, Ph.D. thesis, Freie Universität Berlin 2009.

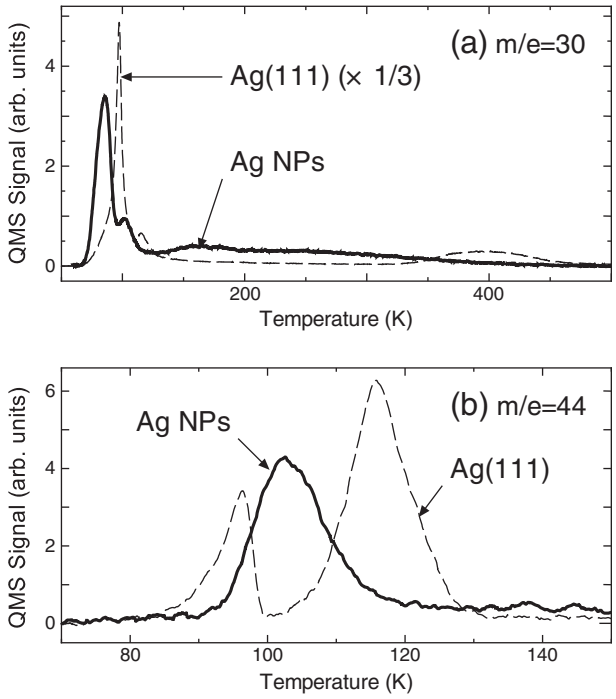

Fig. 1. (a) TPD results measured at m/e = 30 from 8-nm Ag NPs/Al_2O_3/NiAl(110) (thick solid curve) and Ag(111) (dashed curves, multiplied by 1/3) after saturating either surface with NO at 75 K. (b) Corresponding TPD results measured at m/e = 44.

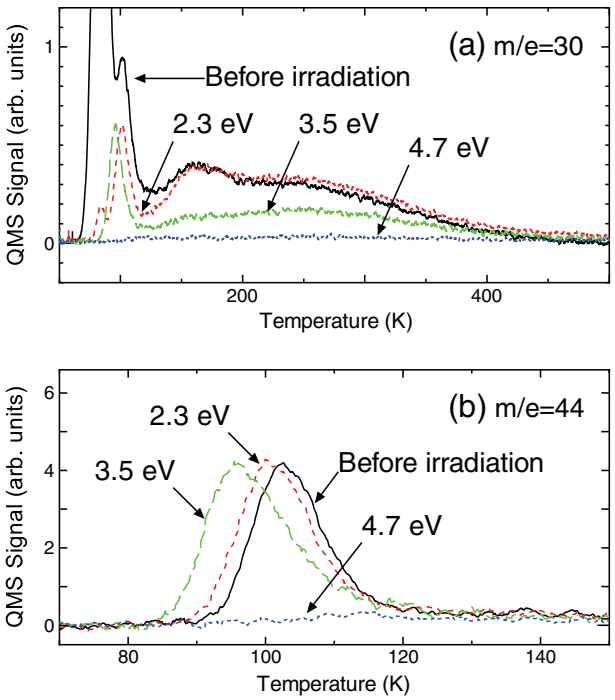

Fig. 2. (a) TPD results measured at m/e = 30 from 8-nm Ag NPs/Al_2O_3/NiAl(110) after saturating with NO at 75 K, before (black solid curve, the same data as in Fig. 1) and after irradiation at 2.3 eV (red short dashed), 3.5 eV (green dashed), and 4.7 eV (blue dotted). (b) Corresponding data measured at m/e = 44. The post-irradiation TPD was performed after PID of NO (see Fig. 3) had been depleted by prolonged irradiation.

monomers.[22] We designate NO molecules desorbing from NO dimers as NO-α, and those from NO monomers as NO-β, respectively.

Fig. 1(b) shows TPD results measured at m/e = 44 (N_2O) simultaneously with those at m/e = 30 shown in Fig. 1(a), from Ag NPs and Ag(111). No desorption signal is observed above 140 K for either surface. Again, the peak at 102 K for Ag NPs and that at 115 K for Ag(111) are assigned to desorption of N_2O whose NO fragments appear at m/e = 30. The 95-K peak observed in the Ag(111) spectrum is attributable to N_2O desorbing concurrently with the decomposition of less stable NO dimers with certain structures observed by STM.[20] No corresponding peak is seen for Ag NPs; so this less stable type of NO dimers is absent on them. This leads to differences in the branching ratio between NO-α and NO-β; the signal intensity ratio of NO-β to NO-α is ~2.3 times larger for Ag NPs than for Ag(111). The N_2O signal intensity compared to the total amount of NO signal (NO-α + NO-β) is also slightly higher for the Ag NPs.

As a control experiment a TPD measurement of NO dosed at 75 K on a bare Al_2O_3/NiAl(110) surface was performed. Neither parent NO molecules nor other possible products such as N_2O, NO_2, N_2, O, or O_2 were detected. This confirms that NO sticks preferentially on the Ag NPs at 75 K and does not adsorb on the Al_2O_3 surface at 75 K. This fact allows us to investigate thermal and photoreactions of NO adsorbed only on the surface of the Ag NPs.

Based on these TPD results of desorption peaks of NO-α, NO-β, and N_2O on the Ag NPs, effects of irradiation of NO dimers on the Ag NPs were investigated by post-irradiation TPD measurements. The sample was irradiated with 2.3, 3.5, or 4.7 eV photons until photodesorption of NO almost ceased, indicating depletion of reactive species. The required total irradiances were ~10^{19} photons/cm^2. The remaining adsorbates were then analyzed by TPD.

Fig. 2(a) displays post-irradiation TPD spectra detected at m/e = 30. The NO-α peak at 86 K was completely depleted at 3.5 and 4.7 eV; at 2.3 eV, a tiny peak of NO-α remained. The intensity of the peak assigned to N_2O at ~100 K was reduced to about 2/3 at 2.3 and 3.5 eV. The broad feature from 120 K to 450 K stemming from NO-β was almost unchanged at 2.3 eV, whereas it was depleted by more than half at 3.5 eV. The decrease of peak intensity at 160 K is larger than that at 250 K. At 4.7 eV, all the peaks were absent, indicating that NO dimers (giving rise to NO-α), NO monomers (NO-β), and N_2O were all totally depleted by irradiation at this photon energy.

The post-irradiation TPD spectra detected at m/e = 44 in Fig. 2(b) confirm these assignments. The N_2O peak at 102 K in the pre-irradiation TPD was shifted to lower temperature by 2 and 7 K after 2.3 and 3.5 eV photoirradiation, but its intensity was almost unchanged. In contrast, the N_2O peak disappeared after 4.7 eV photoirradiation. These results are consistent with our direct study of adsorbed N_2O[26] : N_2O on Ag(111) is photoinert at 2.3 eV, slightly photoreactive at 3.5 eV, and fully depleted at 4.7 eV. Note that the presence of the N_2O peak in the post-irradiation TPD spectra after 2.3 and 3.5 eV irradiation shows clearly that the photoeffects reported are not caused by transient heating of the NPs, in agreement with estimates of the temperature increase by 2 mJ/cm^2 laser pulses (<10 K).

We note that the threshold photon energy for photoreactions of NO dimers, NO monomers, and N_2O were the same on the Ag NPs and on Ag(111).[26,28] Also, post-irradiation TPD showed no differences if depletion of reactants was carried out with *p*- or *s*-polarized light.

3.2. Photo-induced desorption (PID)

The efficacy of photoreactions of adsorbed NO dimers was investigated by measuring PID of the photoproduct NO as a function of photon energy and light polarization. If the PCS is independent of coverage, the PID signal intensity scales with the coverage of reactants, and it should decay exponentially with irradiation in the case of one-photon processes. Then the PCS, σ (cm^2), can be evaluated

[28] R. T. Kidd, D. Lennon, and S. R. Meech, J. Phys. Chem. B **103** (1999) 7480.

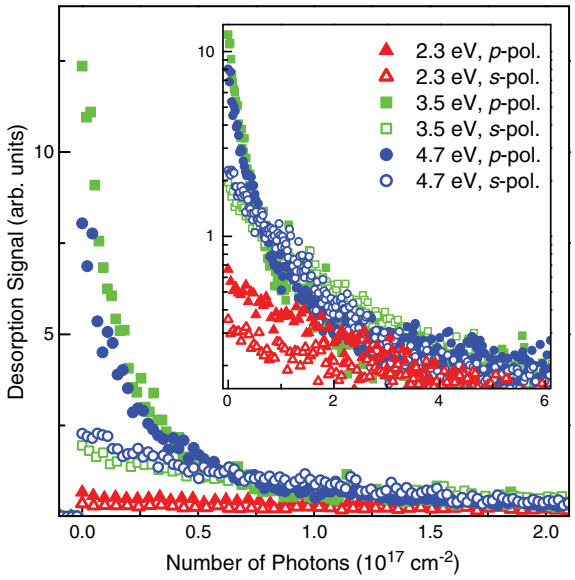

Fig. 3. (color online) PID of NO from NO/8-nm Ag NPs photoexcited at 2.3 eV (triangles), 3.5 eV (squares), and 4.7 eV (circles), in *p*- (solid symbols) and *s*- (open symbols) polarization, respectively. Laser irradiances were ~1.0 mJ/cm^2 per shot for the data at 3.5 eV in *p*-polarization and ~1.7 mJ/cm^2 per shot for the others. Inset shows corresponding semilogarithmic plots for an extended number of photons. Temperature of measurement: 30 K.

by fitting the PID signal I to $I = I_0 \exp(-\sigma N_{ph})$, where I_0 is the initial PID signal and N_{ph} is the irradiance (accumulated number of photons per cm^2). The data points between the maximum and the half maximum were used for fitting in this study; for the reason see below.

Fig. 3 presents PID data of NO (m/e = 30) from the NO dimer on the Ag NPs at 2.3, 3.5, and 4.7 eV in *p*- and *s*-polarization up to $N_{ph} = \sim 2 \times 10^{17}$ photons/cm^2. The inset shows the same data in an extended N_{ph} range up to $\sim 6 \times 10^{17}$ photons/cm^2 in a semilogarithmic plot.

It is obvious that at 3.5 eV in *p*-polarization the PID signal was strongest and decayed fastest, i.e., the PCS was largest. In contrast, only a modest intensity and a much slower decay were observed at 3.5 eV in *s*-polarization. Such a selective enhancement was not seen for PID results on Ag(111) (not shown, see[27]) where the PCS monotonously increased with increasing photon energy, and the observed minor PCS enhancement between *p*- and *s*-polarized light was consistent with the light absorbance of bulk silver.[22,29,30]

The semilogarithmic plots of the PID data (in the inset of Fig. 3) reveal a slowdown of photoreactions for large N_{ph} at 3.5 and 4.7 eV. For example, at 4.7 eV (*p*-pol.) the slope decreases by about an order of magnitude above $N_{ph} = \sim 3 \times 10^{17}$ photons/cm^2, indicating a change of process. This is the reason why the data points between maximum and half-maximum signal were used for the evaluation of the PCS of NO dimers, as mentioned earlier. The change in PCS reflects the change in reactants; the fast initial decay stems from depletion of NO dimers and is followed by slow decay of the photoproduct NO monomers which are much less photoreactive than NO dimers.[23] As was seen in the post-irradiation TPD result in Fig. 2, NO monomers are not photoreactive at 2.3 eV; therefore the PID data at 2.3 eV show only a single exponential decay. It should be noted that monomeric NO contributes negligibly to the initial signal decay; indeed, fitting by a single exponential function gave little difference for the PCS of NO dimers from fitting to a sum of two exponential functions.

[29] N. Nilius, A. Corper, G. Bozdech, N. Ernst, and H.J. Freund, Prog. Surf. Sci. **67** (2001) 99.

[30] K. Watanabe, K. H. Kim, D. Menzel, H.-J. Freund, in preparation.

Table 1
Photodesorption cross sections (PCSs) of NO from 8-nm Ag NPs and Ag(111) dosed with NO at 75 K measured at 2.3–4.7 eV (errors of PCS are between 3 and 25%, with larger values more accurate).

Photon energy (eV)	Polarization	PCS (10^{-18} cm^2)				Enhancement factor, ratio (a) to (b)
		(a) 8-nm Ag NPs		(b) Ag(111)		
		PCS	p/s ratio	PCS	p/s ratio	
2.3	*p*	2.1	1.5	0.86	2.2	2.4
	s	1.4		0.39		3.6
3.5	*p*	59	8.0	3.9	1.4	15
	s	7.3		2.8		2.6
4.0	*Non-pol.*	9.5	N/A	5.8	N/A	1.6
4.7	*p*	38	3.5	15	1.3	2.5
	s	11		12		0.9

Therefore, data obtained from single exponential fitting of the PID datasets in Fig. 3 represent the PCS values of NO dimers.

Table 1 summarizes the PCS values of NO from NO dimers adsorbed on the Ag NPs and on Ag(111), obtained from PID measurements similar to and including those in Fig. 3. Typical errors were up to about 8% and 25% for the results with *p*- and *s*-polarizations, respectively. A gradual increase of the PCS from 8.6×10^{-19} to 1.5×10^{-17} cm^2 with increasing photon energy can be seen for the Ag(111) results with *p*-polarized light, whereas a distinct maximum of 5.9×10^{-17} cm^2 is found at 3.5 eV in *p*-polarization for the Ag NPs.

The ratios of PCSs between *p*- and *s*-polarization, also given in the table, are between 1 and 3 except for the result at 3.5 eV in *p*-polarization, where it is ~8. Also, in the ratios of PCSs between the Ag NPs and Ag(111) an extraordinary enhancement is obvious at 3.5 eV in *p*-polarization, whereas only a 2–3 fold enhancement is generally found for the Ag NPs at other photon energies, except for 4.7 eV in *s*-polarization. The remarkable dependences on polarization and photon energy of PCSs at 3.5 eV point to an additional enhancement mechanism due to the excitation of the (1,0) mode of Mie plasmon, [25,31] as will be discussed later.

When PID was measured while keeping the sample temperature at 130 K so that NO dimers do not exist on the surface, only a very slow decay similar to that found for large N_{ph} ($> 3 \times 10^{17}$ cm^{-2}) was observed, even at 3.5 and 4.7 eV. This confirms that NO dimers are responsible for the fast initial decay in Fig. 3, and monomers for the slow late decay. The monomer PCSs derived from the late decay of signal were generally between ~20 and 40 times smaller than the dimer values in Table 1. Because of their smallness they were much less accurate; they are not given it detail, therefore. It was clear, however, that the trends with photon energy and the changes induced by the NPs are similar to those for the dimers. Specifically, there is a considerable plasmon enhancement – at 3.5 eV the ratio of PCSs in *p*- and *s*-polarization on the NPs was even larger (about 20) for the monomers than the dimers, and the ratio of PCSs for monomers on NPs and Ag(111) (3.5 eV, *p*-pol) was also larger (~18). This may be connected with the environmental changes of the monomers on Ag NPs (see below). Semiquantitatively the same NP influences on the PCSs can be stated for the monomers as for the dimers.

3.3. Mass-selected time-of-flight (MS-TOF)

Translational energy distributions of photodesorbed NO were measured by means of the MS-TOF method to investigate the photodesorption dynamics. Fig. 4 displays normalized TOF spectra of NO photodesorbed from Ag NPs and from Ag(111). The upper panel (a) compares spectra taken at 2.3 eV in *p*-polarization up to $N_{ph} = 5 \times 10^{17}$ cm^2 where the main reactant was NO dimers as shown above. The lower panel (b) presents TOF spectra of NO

[31] F. Evers, C. Rakete, K. Watanabe, D. Menzel, and H.J. Freund, Surf. Sci. **593** (2005) 43.

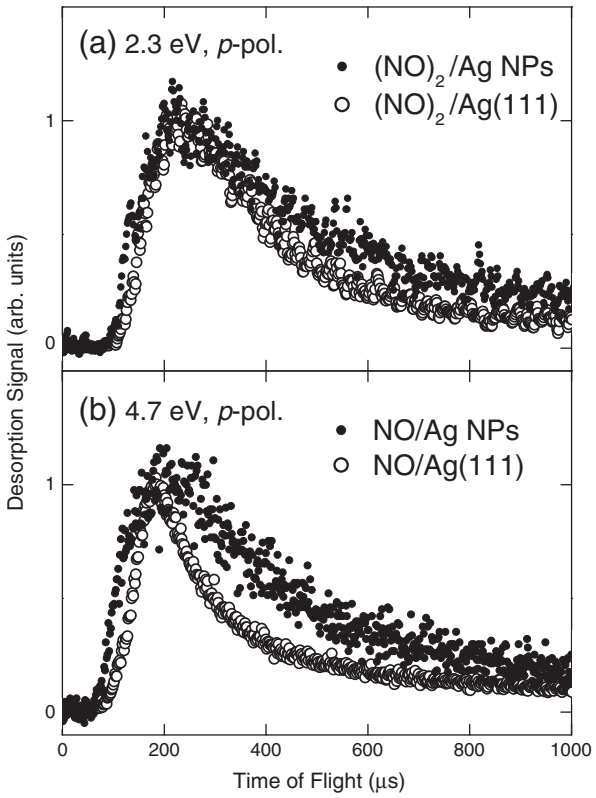

Fig. 4. (a) Normalized TOF spectra of NO photodesorbed from 8-nm Ag NPs and from Ag(111) at 2.3 eV in *p*-polarization accumulated from 0 to 5×10^{17} photons/cm^2, i.e. stemming mainly from NO dimers (see text). (b) Same, measured at 4.7 eV in *p*-polarization but accumulated from 5×10^{18} to 2×10^{19} photons/cm^2, i.e. stemming mainly from NO monomers.

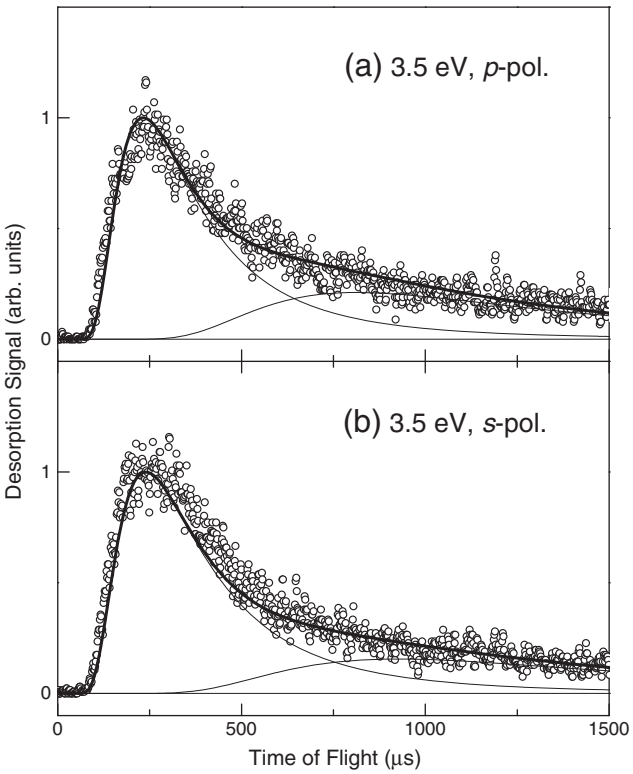

Fig. 5. TOF spectra of NO photodesorbed from NO dimers adsorbed on 8-nm Ag NPs/Al_2O_3/NiAl(110) at 3.5 eV in *p*- and *s*-polarization with irradiances of 1×10^{16} and 1.5×10^{17} photons/cm^2 for (a) and (b), respectively. The thick solid curves are fits to the results by a sum of two shifted Maxwell-Boltzmann distribution functions (see text) shown by thin solid curves.

monomers at 4.7 eV from $N_{ph}=5\times10^{18}$ to 2×10^{19} cm^2 where the initially adsorbed NO dimers had been depleted and only NO monomers are photodesorbed.[32]

The spectra have a single peak occurring at ~250 and ~200 μs in Fig. 4, panels (a) and (b), respectively, indicating that the NO photodesorbed from NO monomers are generally faster than those from NO dimers. As will be shown later, these spectra can be fitted by a sum of Maxwell-Boltzmann distribution functions with different mean translational energies. Two other notable observations are that the TOF peaks in the spectra of the Ag NP results are broader than those of Ag(111), and that the peak in the NO deriving from dimers is much broader than that in the NO monomer results, especially on Ag(111).

Fig. 5(a) and (b) show TOF spectra of NO photodesorbed from NO dimers adsorbed on Ag NPs with 3.5 eV photons in *p*- and *s*-polarization with irradiances of 1×10^{16} and 1.5×10^{17} photons/cm^2, respectively. As mentioned in the previous section, these small irradiances ensure that the main source was NO dimers. We recall that irradiation at 3.5 eV in *p*-polarization excites the (1,0) mode of the Mie plasmon of Ag NPs, whereas irradiation in *s*-polarization does not couple to the plasmon resonance.[25,33]

The TOF spectra are fitted by a sum of two shifted flux-weighted Maxwell-Boltzmann distribution functions,[19] $f(t)=a/t^4\exp(-b(L/t-v_0)^2)$, where a, b are the parameters of amplitude and spread, respectively, t the flight time of desorbate, L the flight length (~19 cm), and v_0 the parameter related to the shift from the thermal Maxwell-Boltzmann distribution. The mean translational energy $\langle E_{tr}\rangle$ was obtained by numerical integration of the fitted function and can be expressed by the translational temperature, $T_{tr}=\langle E_{tr}\rangle/2k_B$, where k_B is the Boltzmann constant.

The T_{tr} of the slow component is even lower than the thermal desorption temperature of the NO on Ag surfaces. Thus, this component can be ascribed to secondary processes among adsorbates/desorbates or scattering of the molecules in the flight tube and ionizer walls, and is insignificant in our context; so it is not considered further. The T_{tr} of the fast components in the spectra of Fig. 5(a) and (b) were found to be 690 and 680 K, respectively. These values as well as the overall spectral features are identical within the experimental error.

Fig. 6 shows evolutions with irradiance of T_{tr} of the fast NO component photodesorbed from Ag NPs and from Ag(111) at 2.3, 3.5, and 4.7 eV in *p*-polarization. Data measured at 3.5 eV in *s*-polarization are also shown. On Ag(111), T_{tr} increases with N_{ph} from ~600 K and levels off at ~650 K for 2.3 eV and at ~900 K for 3.5 and 4.7 eV. These changes in T_{tr} are attributable to the conversion of reactants from part of the initially adsorbed NO dimers to NO monomers. As was seen in the post-irradiation TPD results in Fig. 2(a), NO monomers are partially and totally photoreactive at 3.5 and 4.7 eV, respectively. Thus, the initial T_{tr} values of ~600 K and the converging T_{tr} values of ~900 K at large N_{ph} correspond to NO stemming from NO dimers and NO monomers, respectively. Their superposition leads to the transition of T_{tr} values at intermediate N_{ph} which therefore reflects the change of relative coverage between NO dimers and monomers. The increase of T_{tr} at 4.7 eV is faster than that at 3.5 eV because the PCS is larger at 4.7 eV than at 3.5 eV. At 2.3 eV, in contrast, T_{tr} increases from ~580 K to 640 K, then levels off at 630 K. At 2.3 eV, NO dimers react to form NO monomers, but the latter are not photoreactive.

[32] At low surface temperatures (below ~75 K), NO dimers can be re-dimerized from NO monomers produced during the photodesorption measurements, though the coverage is small. This process will be described in ref. 30.

[33] W. Drachsel, M. Adelt, N. Nilius, H. -J. Freund, J. Electr. Spectrosc. Relat. Phenom. **122** (2002) 239.

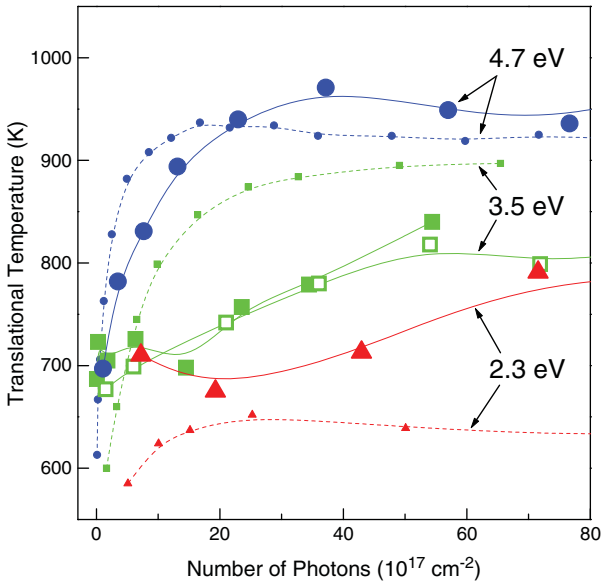

Fig. 6. (color online) Evolutions of translational temperatures of photodesorbed NO from 8-nm Ag NPs/Al_2O_3/NiAl(110) (symbols + solid curves) and from Ag(111) (smaller symbols + dashed curves) excited at 2.3 eV (triangles), 3.5 eV (squares), and 4.7 eV (circles) in *p* polarization. Open squares show results at 3.5 eV in *s* polarization. The curves are guides to the eye.

The slight change in T_{tr} at 2.3 eV can be attributed to photoreaction-induced changes in the adsorption states of NO dimers.[32]

A similar evolution is seen for the results from the Ag NPs (shown as larger symbols) photoexcited at 4.7 eV; T_{tr} values increased from ~700 K to ~950 K. However, the rise is slower than on Ag(111) despite the larger PCS. The T_{tr} behave very differently from Ag(111) at 2.3 and 3.5 eV: they stay at ~700 K in the early stage, then rise slowly and level off at ~800 K. Leveling-off of T_{tr} occurs much later, above $N_{ph} = 6\times10^{18}$ cm^2. This is not consistent with the PID results in Fig. 3, where initially adsorbed NO dimers on the Ag NPs appear to be depleted already at $N_{ph} = 1\times10^{18}$ cm^2. Also, with 3.5-eV photoexcitation T_{tr} reached only ~800 K on the Ag NPs while it rose to nearly 900 K on Ag(111). This indicates that adsorption states and therefore photodesorption dynamics of NO monomers at 3.5 eV on the Ag NPs are modified from those on Ag(111) as also suggested by the remarkable difference in the TPD results shown in Fig. 1. This will be discussed below.

4. Discussion

The objective of the present work is to investigate and interpret differences between flat and particulate metal surfaces (here Ag as an example) in photoinduced processes, and to explore possibilities of tuning and enhancing photochemistry. Factors expected to control photochemistry on single-crystal metals and supported metal nanoparticles can be summarized as follows (after Table 1 of ref.[6]):

(a) geometric structure,
(b) electronic structure,
(c) chemical properties,
(d) optical properties,
(e) energy transport in the substrate,
(f) particle–particle interactions.

These factors will contribute in different ways to each elementary process. Generally, photochemical processes at metal surfaces can be well understood in terms of semiclassical mechanisms (MGR and its variations[15,16,34]). In the present case all previous work[21,28] and our own results[9,23] agree that photodesorption is of the substrate mediated type, and that the transient negative ion (TNI) mechanism[19] is predominant. Its steps are

(1) photoabsorption by the metal substrate,
(2) creation of electron–hole pairs,
(3) transport of hot carriers to an adsorbate and attachment to it, leading to its electronic excitation,
(4) nuclear motion along the excited state potential energy surface (PES),
(5) de-excitation of adsorbates by back-transfer of hot carrier to the substrate at a different geometry,
(6) nuclear motion along the ground state PES.

Chemical bond cleavage and/or formation can take place on both the excited and/or the ground state PES's.

On this basis we will discuss effects on the following features in the present experimental results related to the influences (a)–(f):

Adsorption states:	(a), (b), (c)
Excitation mechanisms:	(a), (b), (d), (e), (f)
Photoreaction kinetics:	(a), (b), (c), (d)
Photodesorption dynamics:	(a), (b), (c), (d)

4.1. Adsorption states of NO and N_2O on Ag NPs vs Ag(111)

The thermal and photo-induced products formed from NO dimers on Ag NPs and Ag(111) were recorded by TPD at m/e = 30 (NO) and m/e = 44 (N_2O). No other products were detected, e.g. at m/e = 32 (O_2). Therefore we focus on the adsorption states and thermal reactions of NO dimers and their products, NO monomers and N_2O, and discuss the differences between particulate and flat surfaces.

The pre-irradiation TPD results from the Ag NPs and Ag(111) shown in Fig. 1 indicate that initially adsorbed NO dimers react thermally to form NO and N_2O by reactions as reported in[21]

$$(NO)_2 \rightarrow 2NO(a \text{ or } g) \quad (<100\ K) \qquad (R1)$$

$$(NO)_2 \rightarrow N_2O(a \text{ or } g) + O(a) \quad (<130\ K) \qquad (R2)$$

where NO(a) is stabilized by O(a).[28]

Adsorbed NO(a) and N_2O(a) desorb to the gas phase at higher temperatures by,

$$NO(a) \rightarrow NO(g) \quad (> 120\ (300)\ K \text{ on Ag NPs } (Ag(111)) \qquad (R3)$$

$$N_2O(a) \rightarrow N_2O(g) \quad (<130\ K) \qquad (R4)$$

A qualitative difference between Ag NPs and Ag(111) was observed in the thermal reaction R2 of NO dimers. TPD at m/e = 44 showed only a single peak at 102 K on Ag NPs but two peaks at 95 K and 115 K on Ag(111). As mentioned earlier, the 95-K peak on Ag(111) is due to N_2O fragmentation in the ion source, i.e., it is attributable to desorption of N_2O in reaction R2 of NO dimers in less stable phases. It is important to note that this N_2O is stabilized by coadsorbed oxygen atoms, as indicated by experiments with pure N_2O.[26] The STM study[20] showed four phases of $(NO)_2$ (labeled α, β, χ, and δ) coexisting on Ag(111) above 65 K. The α, χ, and δ phases decompose and desorb as NO-α and N_2O at ~95 K; the $(NO)_2$-β phase remains up to ~125 K where all N_2O products desorb. The N_2O peak in the Ag NP spectrum at 102 K corresponds to the 115-K peak in the Ag(111) spectrum. This suggests that only a phase similar to $(NO)_2$-ß is formed on the NPs. Direct STM observations or spectroscopy of $(NO)_2$ on Ag NPs are desirable for more details.

The peak temperatures in the Ag NPs spectra were generally lower than those on Ag(111). We will discuss the two cases separately, namely, weakly bound NO-α and N_2O, and strongly bound NO-β.

[34] P. R. Antoniewicz, Phys. Rev. B **21** (1980) 3811.

Previously we reported that the TPD peaks of NO-α and N_2O from the Ag NPs shift linearly with $1/R$ (R is the particle radius) and approach the peak temperatures on Ag(111) with increasing R.[9] As in the simplest approximation the TPD peak temperature is (roughly) proportional to the binding energy of the adsorbate, this indicates that the adsorption energy decreases with decreasing particle size. This is most easily understood for physisorbed species, because for them the dispersion forces integrate over all atoms in the NP.[9,35] The mean particle size in the present study was 8 nm and the peak temperatures are consistent with the results in ref. [9]. We note that the Ag NPs in the size range of 2 – 10 nm have always a dome-like shape with aspect ratio ~0.5.[25,29] The simple scaling law suggests that changes in surface structure of the NPs do not appear to be important for the observed size dependence.

The TPD features of NO-β on Ag NPs at m/e = 30 are changed considerably from those on Ag(111). On the NPs desorption of NO-β occurs from 120 K to 450 K with peaks at 160 K and 250 K whereas it occurs at much higher temperatures on Ag(111), peaking around 400 K. The NO-β peak has been assigned to decomposition of NO_2(a) formed by NO(a) + O(a) by Ludviksson et al.[36]; Meech's group concluded that it originated from monomeric NO perturbed by O(a).[28] In both interpretations NO-β is thought to be a NO species interacting with surface oxygen atoms, and the presence of O(a) is decisive for the stability of NO "monomers".

The changed NO-β desorption temperatures on Ag NPs compared to Ag(111) could be due to changes in geometry, electronic structure, and/or chemical properties. Ag NPs certainly possess a wider variety of surface sites compared to Ag(111). No crystalline facets have been resolved with STM,[25,29] and the dome-like shapes will lead to varied orientations and densities of the actual surface. Furthermore, there are boundaries to the Al_2O_3 substrate. All this should lead to a broad distribution of binding energies of NO-β; the distribution in particle sizes may further increase the diversity in binding energies. Also, the chemical interaction with oxygen atoms may be different between the Ag NPs and Ag(111). As the former possess more open surfaces and small particles can be deformed more easily, surface oxygen atoms may migrate subsurface more easily. This makes it understandable that NO-ß is destabilized on Ag NPs, leading to desorption at lower temperatures.

The broad feature of NO-β desorption could in principle indicate structural changes of the Ag NPs by heating, as metal nanoparticles deposited on the Al_2O_3 layers can undergo aggregation and diffusion into the substrate by annealing at temperatures above ~600 K.[37] However, no change in the TPD spectra of NO-β was observed in at least three cycles of TPD measurements up to 550 K after a single preparation of Ag NPs. Thus we can conclude that the structure of the Ag NPs is stable up to 550 K.

So the main differences between the Ag NPs and Ag(111) concerning adsorption states of NO dimers and monomers can be summarized as follows: (1) The binding energy of NO dimers on the Ag NPs is about 10% lower than on Ag(111). On the Ag NPs only the most stable β-phase $(NO)_2$ appears to exist after preparation at 75 K. (2) The thermal stability of NO monomers on the Ag NPs is considerably reduced, and the adsorption sites are much more inhomogeneous than on Ag(111). (3) N_2O coadsorbed with O is also more weakly bound on Ag NPs than on Ag(111).

Concerning the photoreactions of NO dimers and monomers, it is important to note that the samples were photoirradiated at ~30 K. Thus, the inhomogeneity in their adsorption states under/after irradiation might be smaller before heating for TPD.

Finally we stress that we did not observe associative desorption of O_2 from either Ag NPs or Ag(111). This is in contrast to the observations of other groups[21,22] who saw O_2 desorbing from NO/Ag(111) at 600 K. We believe that in our NP samples diffusion of surface oxygen atoms to subsurface sites occurs more easily.

4.2. Excitation mechanisms

Based on PCS measurements as functions of incident angle and polarization, the photoexcitation mechanism in the NO/Ag(111) system has been determined by the groups of Ho[21] and Meech[28] to be of the substrate mediated type, more specifically to proceed via adsorbate excitation by hot electron attachment from the metal to create a TNI. Judging from the generally monotonic increase of the PCS with photon energy except for the enhancement at 3.5 eV in *p*-polarization on Ag NPs,[21,28] and the similar translational temperatures of NO from Ag NPs and Ag(111), it is very probable that the same mechanism dominates also on the NO/Ag NPs. Direct photoexcitation of NO dimers in the gas phase requires photon energies higher than 5.2 eV,[38] which is beyond our highest photon energy (4.7 eV). This excludes direct excitation of the adsorbate. The TPD results showed no evidence of qualitative differences in the adsorption states of NO dimers between the Ag NPs and Ag(111) besides the general slight decrease of adsorption strength on the NPs. Also, the detailed results obtained recently[24] on the internal state energy distributions of photodesorbed NO stress the equality of responsible excitations for single crystal and NP surfaces and their compatibility with the TNI mechanism. Thus, it is warranted to compare the PCS values on Ag NPs and Ag (111) on equal footing. The seen changes must then be due to particle properties. In terms of the steps of the TNI mechanism given above, only steps (1) to (3) can differ between the Ag NPs and Ag(111). The efficiency of the photon absorption step (1) should be determined by the absorbance of silver regardless of the morphology of substrate, i.e. flat or particulate, if there is no special optical mode like a plasmon. The probability that absorbed light is converted to hot carriers (step (2)) could be influenced by particle properties, as could be step (3), transport of hot carriers to adsorbates and transfer into them.

The PCS of NO dimers on the Ag NPs was found generally to be 2 to 3 times higher than those on Ag(111). At 3.5 eV in *p*-polarization, the PCS was even enhanced 15-fold (see Table 1). This latter large PCS enhancement is attributable to the excitation of the (1,0) mode of the Mie plasmon of the Ag NPs which lies at 3.5 to 3.6 eV.[25,31] The (1,0) mode is excited only by the electric field along the surface normal. Indeed, photoirradiation at 3.5 eV in *s*-polarization resulted in an enhancement factor of only 2.6, corroborating that at this polarization the (1,0) mode was not excited (see Table 1). This is also borne out by the large *p*/s ratio of ~8 for Ag NPs at 3.5 eV compared to 1.4 for Ag(111) which is consistent with the absorbance change.

The role of plasmon excitation in increasing the PCS is primarily due to the enhancement of the local electric field at and near the NP surface, leading to an increase of the number of hot electrons produced per incoming photon. The fact that the yield of the 2PPE (two-photon photoemission) signal from Ag NPs on Al_2O_3/NiAl(110) has been found to be significantly enhanced and peaked at 3.6 eV in *p*-polarization[31] is consistent with this conclusion. Therefore the observed enhancement of the PCS can be explained by the increased hot electron yield[39] due to the enhanced electric field at the surface (antenna effect).[40] We note that the (1,1) mode of the Mie plasmon at about 2.3 eV which in principle could be excited in

[35] J.-H. Fischer-Wohlfahrt et al., Phys. Rev. B **81** (2010) 241418.
[36] A. Ludviksson, C. Huang, H. J. Jansch, R. M. Martin, Surf. Sci. **284** (1993) 328.
[37] M. Bäumer and H. -J. Freund, Progr. Surf. Sci. **61** (1999) 127.
[38] O. Gessner et al., Science **311** (2006) 219.
[39] R. Monreal and S. P. Apell, Phys. Rev. B **41** (1990) 7852.
[40] P. Mühlschlegel, H. J. Eisler, O. J. F. Martin, B. Hecht, and D. W. Pohl, Science, **308** (2005) 1607.

s-polarization is quenched by screening by the close-by NiAl(110) substrate.[33]

For particles larger than ~20 nm, plasmons decay predominantly by luminescence, i.e. by photon re-emission.[4] With decreasing particle size, decay into electron–hole pairs via Landau damping increasingly competes.[41] Hot electrons so formed can then play a role in photochemistry, in addition to those produced directly by photoabsorption, and this will increase the PCS. Indeed our size-dependent data of photodesorption of NO published earlier[9] corroborate this. This coupling of plasmon excitation with electron–hole pair creation can also occur more directly by so-called chemical interface damping (CID) which couples the plasmon energy into adsorbate excitations.[42] Both paths can lead to temporary electron attachment to the adsorbate, i.e. formation of TNI (transient negative ions) in the substrate mediated excitation mechanism.[18,19] Together, these paths can explain the large enhancement factor. On the other hand, the fact that there was no change of the translational energy distribution (and also of internal energy distributions[24]) of photodesorbed NO on and off the plasmon resonance (Fig. 5) implies the absence of any direct influence of the plasmon excitation which would lead to different dynamics. Such an effect has been suggested to explain photodesorption of adsorbed Xe on Ag NPs.[11] We conclude that NP plasmons have a strong effect on steps (1) and (2) of the TNI mechanism.

For the PCS enhancement factors of 2–3 for Ag NPs vs. Ag(111) off the plasmon resonance, plasmons cannot play a role, and photon re-emission should be negligible considering the small size of our NPs. In contrast, the efficiency of step (3), transport of hot electrons from inside the substrate to the surface, will depend on the particle radius R, when R is smaller than the mean free path λ of hot electrons.[43] When $R<\lambda$, the PCS should scale with the volume to surface ratio, i.e., $\sigma \propto 1/R$. This behavior was indeed found previously.[9]

The electron mean free path λ is given by $\lambda_{e-e}=\tau \cdot v$, where τ is the hot electron lifetime and v the electron velocity. The electron affinity level of NO dimers on Ag (111) is located ~2 eV from the Fermi level.[44] At 2 eV λ_{e-e} is ~8 nm with $\tau = 5$ fs[45] and $v = \sim 1.6\times10^6$ *m/s*.[46] The average height of the Ag NPs is ~2 nm (with an aspect ratio of height to radius of 1:2). As a result, the hot electrons will be reflected several times at the surface and the interface between the NP and the alumina film before dissipating sufficient energy (via electron–electron and interfacial scattering) that they cannot enter the adsorbate LUMO any more. In this way the flux of ballistic hot electrons to the adsorbate will increase on Ag NP compared to flat Ag(111). In the latter case, roughly half of the hot electrons will collide with the surface about once; the other half disappears into the bulk. While this is a very crude estimate it shows the qualitative effect and even agrees with the observed order of magnitude. More detailed modeling would be needed to better quantify this estimate.

This reasoning is valid for delocalized electrons in the *sp*-band for which the number of produced hot electrons per NP and laser pulse – and therefore the desorption signal – scales with R^3 whereas the number of adsorbates scales with R^2; this leads to a scaling of the PCS with $1/R$. These excitations are the only ones accessible at 2.3 and 3.5 eV. For excitations by localized hot holes such as those in *d*-bands, or for direct excitations from an adsorbate HOMO to the empty *sp*-band (both called TPI mechanism in ref.[9]) both possible at 4.7 eV, we get different scaling; the number of excitations (and the desorption signal) scales with the surface area (i.e., the number of *d*-holes near the surface), and so does the number of surface-localized species, so that the PCS becomes constant with size. The relative signal intensities determine which path is predominantly seen, while the measured signal decay monitors the path with the largest PCS. Therefore, the localized excitations (TPI) can be seen most easily at small sizes,[9] even though the PCS measured may be that caused by the delocalized excitations (TNI), if this is larger.

We conclude that the minor PCS enhancements seen for Ag NPs vs. Ag(111) if plasmon excitation can be ruled out are due to hot electron confinement in the NPs which increases their collision number with adsorbate LUMOs. We mention that we recently saw another confinement effect in nonlinear enhancements of PCSs in the same system when using femtosecond (~100 fs) excitation at 3.1 eV.[47]

As to the excitation that leads to photodesorption of NO-ß from the monomers and NP effects on it, we will discuss this below in connection with the monomer evolution.

4.3. Photodesorption dynamics

The translational energy distributions of photodesorbed molecules result from details of potential energy surfaces of adsorbate-surface interactions, lifetimes of excited states, etc.[18,19] From state-resolved studies of photodesorption dynamics of NO in the same system[24] we concluded that the mechanisms of photoexcitation and photodesorption are the same for NO dimers on Ag NPs and on Ag(111), although the adsorption strength and the PCS depend on the particle size. The similarity of MS-TOF spectra of NO from NO adsorbed on the Ag NPs and Ag(111) in the present study (Fig. 4) agrees with these conclusions. The peaks of the MS-TOF spectra are located at almost the same position for both substrates, and the estimated mean translational energies are very close. The present work adds information on the weaker channel of NO dimer evolution, the NO-ß species.

The MS-TOF spectra of NO from NO dimers and monomers on the Ag NPs are not only downshifted, but also generally noticeably broader than those from Ag(111). A straightforward explanation of the difference of TOF spectra between Ag NPs and Ag(111) can be based on the differences of the adsorption states (binding energy and sites, interaction with O(ad)) on the two types of substrates. The Ag NPs possess more complex surface structures compared to the (111) face and therefore the adsorption states of NO dimers and particularly of the monomers will be more diverse than those on Ag(111).

The appearance of higher velocity components (i.e., the TOF signal rising earlier than the peak) of NO from Ag NPs shown in Fig. 4 could partly be caused by the weaker binding on the ground state PES of NO dimers and monomers for desorbing NO molecules, as less of the total energy stemming from excitation/deexcitation will be needed to escape from the ground state well. However, this should be a small effect, and additional effects are expected. One could be an increase of the lifetime of the adsorbate excited state for Ag NPs compared to Ag(111). This is expected from the weaker bond, as this will make the adsorbate–surface distance longer; the transient electronically excited state can then survive longer before de-excitation due to tunneling of charge back to the metal. This will result in a higher kinetic energy gain on the excited state PES if the slope near the Franck-Condon region is the same.

The lower velocity components in the TOF distributions of NO from Ag NPs compared to Ag(111) can be explained by a similar argument in the opposite direction, assuming deeper ground state potential wells and shorter lifetimes of the electronically excited state of NO at certain sites or environments of the Ag NPs. An additional contribution of slow molecules could stem from a geometrical effect in the case of the Ag NPs. Since the Ag NPs are shaped dome-like,[25,29] some desorbing molecules might be scattered off neighboring NPs

[41] R. A. Molina, D. Weinmann, and R. A. Jalabert, Phys. Rev. B **65** (2002) 155427.
[42] F. Stietz and F. Träger, Phil. Mag. B **79** (1999) 1281.
[43] V. P. Zhdanov and B. Kasemo, J. Phys.: Condens. Matter **16** (2004) 7131.
[44] H. Nakamura and K. Yamashita, J. Chem. Phys. **125** (2006) 084708.
[45] M. Bauer and M. Aeschlimann, J. Electron Spectrosc. Rel. Phen. **124** (2002) 225.
[46] D.R. Lide, *CRC Handbook of Chemistry and Physics, Taylor and Francis, Boca Raton-London-New York 2008.*
[47] K. H. Kim, K. Watanabe, D. Mulugeta, H.-J. Freund, and D. Menzel, Phys. Rev. Lett. **107** (2011) 047401.

and lose energy. At a density of NPs of 4×10^{11} cm^{-2} and a mean diameter of 8 nm, the mean interparticle distance (edge to edge) is about 8 nm. About 10% of total desorbates would then experience collisions with adjacent Ag NPs.[27] In such collisions even secondary reaction processes would appear conceivable. However, no clear evidence of such processes has been seen.

4.4. Photoreaction kinetics

It is an intriguing question how the photoreaction kinetics of NO species is modified by the factors (a) – (d) between Ag NPs and Ag(111). First, we summarize the main photoreaction paths of the NO species. NO dimers and monomers on Ag surfaces irradiated with visible and uv photons undergo photoreactions similar to the thermal reactions mentioned earlier. The main photoreaction paths of NO dimers on the Ag NPs and Ag(111) have been identified based on the post-irradiation TPD and photodesorption measurements[21,22] as

$$(NO)_2 \rightarrow 2NO(a \text{ or } g) \quad (R5)$$

$$(NO)_2 \rightarrow N_2O(a \text{ or } g) + O(a) \quad (R6)$$

Direct photochemical formation of N_2 from NO dimer,

$$(NO)_2 \rightarrow N_2(g \text{ or } a) + 2O(a) \text{ or } O_2(g) \quad (R7)$$

has been recently found on Ag(111) with 2.3, 3.5 and 4.7 eV excitation.[23] As this reaction channel is weak, it was not investigated in the present study.

The NO monomer photodesorbs molecularly,

$$NO(a) \rightarrow NO(g) \quad (R8)$$

Photoreactions of $N_2O(a)$ formed by (R6) were studied in ref.[26] and are not considered in the present study.

The photon energy dependences of photoreactions of NO dimers and monomers on Ag surfaces are different. NO dimers are photoreactive at 2.3 eV and higher as shown by the post-irradiation TPD results in Fig. 2a. This can be understood by the mentioned theoretical calculation[44] predicting that the electron affinity level of the adsorbed NO dimer (its LUMO) is located at ~2 eV above the Fermi level. NO monomers are photoinert at 2.3 eV, partly photoreactive at 3.5 and 4.0 eV, and fully photoreactive at 4.7 eV (See Fig. 2a). Thus, the electron affinity level of the NO monomers responsible for photoreactions must be located above 2.3 eV and spread over the range 3.5 to 4.0 eV, but below 4.7 eV. The locations of the affinity levels of the adsorbed NO dimers and monomers seem qualitatively unchanged between the Ag NPs and Ag(111).

The PID data presented in Fig. 3 contain the conversion from NO dimers to NO monomers; the decay slows down in the late stage of photoreactions. The early and the late parts of the PID signal correspond to NO dimers and monomers, respectively, which was confirmed in ref.[23] The PCS of the NO monomers on Ag(111) is about an order of magnitude smaller than that of NO dimers at 3.5 eV.[22,27,30] The PCSs of NO dimers and monomers in principle determine the kinetics of R5 and R8, respectively.

We recall that the PCS data summarized in Table 1, which show remarkable enhancement by confinement effects and plasmon excitation, were derived from the initial decay of the PID data, ascribable to dimer dissociation/desorption. Therefore, they contain essentially no information about photoreactions of the NO monomers. Such information is contained in the evolution of T_{tr} with irradiance (Fig. 6). It can be seen that T_{tr} generally changes from the characteristic value of NO dimers to that of NO monomers.

However, the change of T_{tr} with irradiance is different for Ag NPs and Ag(111). The initial T_{tr} for Ag NPs is ~100 K higher than for Ag(111). This is attributable to different adsorption strengths of the NO dimers, which change with particle size.[9] The common initial T_{tr} for different photon energies indicates that the photodesorption dynamics of NO from NO dimers is independent of the primary excitation. On the other hand, the final T_{tr} for the Ag NPs is not the same for 4.7 and 3.5 eV; it is ~900 K at 4.7 eV and ~800 K at 3.5 eV. The different T_{tr} values at 3.5 eV of ~800 K on Ag NPs *vs.* ~900 K on Ag(111) strongly suggest that the photoreactivity of NO monomers on Ag NPs is modified compared to that on Ag(111).

At 3.5 eV, only about half of the NO monomers are photoreactive both on the Ag NPs and on Ag(111).[30] A small amount of NO dimers may be re-formed when the coverage of NO monomers is not too low for dimerization[32] (this is also the likely reason for the small NO-α peak after 2.3 eV irradiations, see Fig. 2). In addition, the change of T_{tr} with irradiation is slower for Ag NPs in spite of the larger PCS compared to Ag(111). These differences in the T_{tr} behaviors for Ag NPs and Ag(111) can be due to (1) differences in equilibrium surface concentrations of NO dimers and NO monomers, and (2) differences in photodesorption mechanisms and/or dynamics of NO species:

(1) The lower final T_{tr} can indicate a higher relative coverage of NO dimers compared to NO monomers. This could be due to low-temperature re-dimerization (see above, and[32]) during irradiation. As indicated by the TPD data in Fig. 1, NO monomers on the Ag NPs are much more weakly bound compared to Ag(111), and destabilised at lower temperature. Thus, they may re-dimerize more easily on the NPs. Unfortunately we had no means to determine the relative concentrations of NO dimers and NO monomers during the evolution.

(2) Comparison of the final T_{tr} values on Ag NPs for 3.5 and 4.7-eV excitation suggests that the photodesorption mechanism of NO monomers is different for these photon energies, contrary to Ag(111). The photodesorbed NO from the Ag NPs at 3.5 eV at large N_{ph} ($>10^{18}$ cm^{-2}) probably stems from NO monomers which are more weakly bound — they may be less influenced by coadsorbed oxygen atoms located at low coordination surface sites on the NPs. The affinity level of such weakly bound NO monomers is expected at higher energies compared to that of NO monomers on Ag(111), making them fully accessible with hot electrons excited from the Fermi level at $h\nu = 4.7$ eV but only partially accessible at 3.5 eV. In contrast, NO monomers on Ag(111) are strongly perturbed by coadsorbed oxygen atoms, resulting in lower photoreactivity at 3.5 eV.

The coverage dependent stability of NO monomers interacting with oxygen atoms on Ag(111) has been studied by Vondrak et al.[22] They found that at 3.5 eV only parts of the NO monomers are photoreactive. As the adsorption states of NO "monomers" are influenced by interadsorbate interactions, they may be different from those excited at 4.7 eV; this could modify the photoreaction paths. However, this is not consistent with the fact that NO monomers are photodesorbed less efficiently at 3.5 eV than at 4.7 eV. Thus, it is likely that NO monomers on Ag NPs photodesorb at 3.5 eV with lower translational energies than those photodesorbed at 4.7 eV, due to more complex and strongly interacting chemical environments in which photoinert NO(a) and $N_2O(a)$ as well as O(a) coexist. At 4.7 eV, both NO(a) and $N_2O(a)$ are depleted completely, as shown by the post-irradiation TPD results in Fig. 2.

These details on the photo-induced behavior of NO monomers show that the combination of NP-induced adsorbate properties with the kinetics of their formation and destruction can lead to changed photoreactivity.

5. Summary and conclusions

The thermal and photo-induced reactions of NO adsorbed on ~8 nm Ag NPs on Al_2O_3/NiAl(110) were investigated by temperature programmed desorption (TPD) before and after irradiation, and by photo-induced desorption including mass-selected time-of-flight

(MS-TOF) measurements. All results were compared in situ to the same processes on Ag(111). The main aim of this investigation was to single out particle-induced effects. The TPD results showed that NO dimers and their reaction products interact with the Ag NPs somewhat more weakly than with Ag(111); for the NO “monomers” we find considerably decreased thermal stability and stronger variability on the NPs.

The mechanisms of photoexcitation and photoreactions of NO dimers are essentially unchanged between the Ag NPs and Ag(111), in agreement with previous results. Compared to Ag(111), the photodesorption cross section (PCS) of NO stemming from NO dimers on the Ag NPs is enhanced by a factor of ~3 off the plasmon resonance and by a factor of ~15 at the (1,0) Mie plasmon at 3.5 eV in *p*-polarization, compared to Ag(111). The PCS enhancement without plasmon participation is ascribed to hot electron confinement due to the particle diameter being shorter than the electron mean free path, and to the isolation by the thin Al_2O_3 film. The plasmon effect is attributable to its surface electric field enhancement, and enhanced electron–hole pair creation by plasmon decay (Landau damping) and chemical interface damping. However, the translational energies derived from the TOF results show that no essential difference exists in photodesorption dynamics between excitation on and off the plasmon resonance and even on Ag NPs and Ag(111).

For the NO monomers changes in the relative branching and its dependence on excitation energy are found which suggests a blue-shifted electron affinity level, compared to Ag(111). This influences the dynamics and leads to changes in the photon energy dependent evolution of the "monomer" species. In situ spectroscopic analysis could improve the understanding further.

The observed influences of the morphology and the confinement of hot electrons as well as of plasmon excitation of the Ag NPs on photochemistry of adsorbed NO, and the changed branching into different reaction channels (desorption, reactions to N_2O and NO monomers) demonstrate possibilities to enhance and tune photochemical processes of adsorbed molecules by using particulate metal surfaces instead of flat metal surfaces. While the main effects can be expected on the efficiency of the primary excitation, changes of branching in more complicated systems can also be expected.

Acknowledgements

We thank Walter Wachsmann for very able technical assistance. We acknowledge financial support from the Deutsche Forschungsgemeinschaft within priority program SPP1093 (Dynamik von Elektronentransferprozessen an Grenzflächen), the German–Israeli Foundation (Dynamics of Electronic Processes in a Confined Environment), the Fonds der Chemischen Industrie, and the NEDO International Joint Research Grant on Photon and Electron Controlled Surface Processes.